Polymer Combustion and New Flame Retardants[1]

Takashi Kashiwagi, Anthony Hamins, Kenneth D. Steckler, and Jeffrey W. Gilman
Building and Fire Research Laboratory
National Institute of Standards and Technology
Gaithersburg, MD 20899

Abstract

The combustion of polymers is a complex coupled process characterized by energy feedback from a flame to the polymer surface and subsequent gasification of the polymer to generate combustible degradation products. Energy feedback characteristics for two different burning configurations, pool burning and vertical wall burning, are discussed. Thermal degradation of polymers and heat transfer in polymer samples are briefly discussed in order to determine polymer gasification rates at specified external heat fluxes. Transient burning rates of two polymereric materials, PMMA and Douglas Fir, are calculated in a pool flame configuration for two different diameters and the predicted results are compared with the experimental data. A similar comparison is made for upward flame spread in the corner of a room. To improve the fire performance of polymers, use of a nonhalogenated char-forming flame retardant is suggested, and its benefits are discussed. The fire performance of a newly developed char forming flame retardant additive combination in a variety of polymers is described. Although its flame retardant mechanism has been studied by analyzing the char structure in the presence of the additives using solid-state NMR, at present it is not clearly understood.

Introduction

Today, synthetic polymeric materials are rapidly replacing more traditional materials such as steel and nonferrous metals as well as natural polymeric materials such as wood, cotton, natural rubber, and so on. They also are attractive materials in their own right, posessing unique and valuable physical properties. However, one weak aspect of synthetic polymer materials compared with steel and other materials is that these materials are combustible under certain conditions. Thus, the majority of polymer-containing end products (for example, cables, carpets, furniture) must pass some type of regulatory fire test to help assure public safety. Therefore, it is important to understand how synthetic polymers burn and how to best modify the materials to make them less flammable in order to pass such tests without compromising their uniquely valuable physical properties and also significantly increasing the cost of end products. This paper briefly describes chemical and physical processes occuring in the gas and condensed phases during the combustion of synthetic polymers and methods to reduce their flammability.

Proc. of 7th Annual BCC Conf. on Flame Retardancy; May 1996; Stamford, CT.

Combustion Process

Combustion of synthetic polymer materials is characterized by a complex coupling between condensed phase and gas phase phenomena. Furthermore, the phenomena in each phase consist of a complex coupling of chemical reactions with heat and mass transfer processes. The role of the condensed phase is to supply combustible gaseous products by receiving a sufficient amount of heat from the gas phase, and the role of the gas phase is to feed a small fraction of heat release from the gas phase oxidation reactions back to the material surface. Characteristics of the critical role in each phase are briefly described below.

Gas Phase

The heat release rate is one of the key quantities characterizing the hazard of a material. However, the heat from oxidation reactions in a flame is released in two components; one is convective and the other is radiative. The fraction of each component, the convective fraction X_c and the radiative fraction X_r (normalized by the idealized heat of combustion of the material), depends strongly on the chemical structure of the material. Typical results for a pool flame configuration as a function of fuel mass flux are shown in Fig.1 and Fig. 2 for methane (and natural gas) and acetylene, respectively [1]. The term X_l is the fraction of the idealized heat release, which is fed back to the fuel surface. In these flames, the flame becomes taller and larger with an increase in mass flux. For large size methane (and natural gas) flames, roughly 80% of the heat release is convected away and roughly 20% of the heat release is radiated. A small fraction, about 2-3% of the total heat release, is fed back to the fuel surface. However, for small flames, the radiative fraction of the heat release becomes quite small due to the smaller flame size and the feedback fraction, X_l, increases. For acetylene flames, the radiative fraction increases up to slightly above 30% and the convective fraction decreases to as low as 45%. Combustion efficiency, X_a (the measured chemical heat release ($X_c + X_r$) divided by the idealized heat release), decreases to about 65% with an increase in the fuel mass flux. Unsaturated materials and aromatic materials tend to have similar characteristics as acetylene and their radiative fraction tends to be between 30 and 40% due to an increase in soot particle concentration in their flames. These results show clearly that heat release characteristics and heat feedback rates depend not only on the chemical structure of the materials but also the diameter of a pool flame and the fuel mass flux.

Radiation from the flame to the sample surface is a major heat feedback mode. The measured radiant flux using a miniature radiant flux gauge at the surface of 30 cm diameter methanol, heptane, and toluene pool flames is shown in Fig.3 [2]. Although the methanol flame is blue and does not generate soot particles, there is still a significant amount of radiative feedback by CO_2 and H_2O band emissions. The radiative heat feedback has a non-uniform spatial distribution. The fraction of radiation in the total heat feedback is about 80% at the center and gradually decreases to about 10% at the edge of the methanol pool flame. For the sooty toluene flame, however, this fraction is nearly constant (about 100%) across the pool surface [2]. It appears that the radiative feedback rate from a pool flame might not increase with a pool diameter beyond a certain size due to radiative blanket effects caused by absorption of radiation from the pool flame to the pool surface by the vaporized fuel gas near the pool surface [3]. In order to predict the

energy feedback rate from a pool flame to the fuel surface, a model needs to be able to predict temperature and chemical species distributions in the flame. However, since detailed understanding of chemical reactions with measured kinetic constants of the numerous possible reactions is limited to small alkanes or to a simplified flow field at present, a global approach has been used in the field of fire research. In this approach, a flame is approximated as a homogeneous mixture of combustion products, unburnt fuel, and inert nitrogen with global, uniform values of soot volume fraction, temperature, concentrations of CO_2 and H_2O, and flame height. These values can be calculated from the amount of entrained air flow into the flame, an energy balance between the heat release and the radiative heat loss, an empirically-obtained combustion efficiency or specific heat of combustion, and an empirically-obtained soot volume fraction correlation.

The flame height can be correlated by the non-dimensionalized heat release rate [4]

$$\dot{Q}^* = \dot{Q}/(\rho_0 C_p T_0 g^{1/2} D^{5/2}) \qquad (1)$$

Then, the flame height, Z_f can be expressed as

$$Z_f/D = c\dot{Q}^* \qquad (2)$$

where $\dot{Q}$ is the heat release rate per unit area of the burning surface, ρ is the gas density, C_p is the specific heat, g is gravity, D is a pool diameter and c is a proportionality constant. The subscript $_0$ denotes at ambient conditions. The entrained air flow rate can also be expressed as a function of the non-dimensionalized heat release rate, the combustion efficiency, the radiative fraction, heat of combustion and stoichiometric constant for various heights of pool flames [5]. Using this global approach in the gas phase and (later described) condensed phase, burning rates of horizontally mounted PMMA slabs and Douglas Fir slabs with two different diameters are calculated and compared with experimental results. This comparison will be discussed subsequently.

Another important fire configuration is flame spread up a vertical wall. Previous experimental data indicate that the heat feedback rate distribution with respect to the height of the wall could be correlated more universally with the non-dimensionalized heat release rate, $\dot{Q}^*_L$, than is the case for the pool flame. Here, $\dot{Q}^*_L$ is

$$\dot{Q}^*_L = \dot{Q}_L/(\rho_0 C_p T_0 g^{1/2} L^{3/2}) \qquad (3)$$

where the subscript $_L$ denotes per unit width. The parameter L is the width of the sample. A typical correlation between heat feedback rate and normalized height is shown in Fig. 4 [6]. The results show that heat feedback rate is nearly constant along the surface under the solid flame from the pyrolysis front and then it decreases sharply. A similar correlation was also obtained for flame spread in a vertical corner configuration though here the flame is taller for a given heat release rate [7].

The above approach requires much experimental data to correlate heat feedback rate with the characteristic length scale and heat release rate. However, recently, another approach solving the partial differential equations of continuity, momentum, energy, and chemical species concentrations numerically has been initiated. Although this approach could calculate flame height, heat feedback rate, and many other characteristics, it requires much information regarding chemical reactions and radiative characteristics. Since such detailed information is limited to end products, it might not be practical to apply such an approach to end products. However, it might be quite useful to apply it to well-defined polymer samples to test the accuracy of the method and also to examine the validity of the approximations used in the global approach described above. It is expected that new results based on detailed models will appear in the near future.

Condensed Phase

In order to burn a polymeric material, thermal energy must be added to it to raise its temperature sufficiently to initiate degradation. This energy could be from an external source, in the case of an ignition event, or from an adjacent flame as heat feedback in the case of flame spread and burning. Thermal radiation is the primary mode of energy transfer from the flame to the polymer surface as discussed above except for small samples (roughly less than 10 cm diameter). The amount of energy absorbed by the polymeric material depends on the level and the spectral characteristics of the radiant flux, absorption characteristics of the material, and the material surface reflectance with respect to the emission spectrum of the incident radiation. Generally, as discussed above, the emission spectra of large flames are continuous in the infrared, due to high-temperature soot particles, with additional strong emission bands from H_2O and CO_2 [8]. The absorption spectra of polymeric materials consist of numerous absorption bands in the infrared wavelength region, depending on the vibration modes of the molecular bonds in the polymer structure. However, most theoretical models in the fire research field make the approximation that radiative feedback and external radiation are completely absorbed at the material surface. This approximation tends to predict higher surface temperatures and shorter ignition delay times.

When temperatures near the surface become high, thermal degradation reactions occur and these evolve small gaseous degradation products. The majority of the evolved products from polymers is combustible. Depending on the nature of the polymer, thermal degradation reactions may proceed by various paths. Since there are several recent books and articles describing thermal degradation chemistry in detail [9-11], only an extremely brief discussion is presented here. It has been accepted that the majority of vinyl polymers degrade thermally by a free radical chain reaction path. Free radical chain reactions consist of random or chain-end initiated scission, depropagation, intermolecular or intramolecular transfer, and termination reactions. Polyethylene, PE, is a typical example of a polymer that undergoes scission at random locations on the main chain to yield many smaller molecular fragments. Polystyrene, PS, polypropylene, PP, and polymethylacrylate, PMA, belong to this group. Polymethylmethacrylate, PMMA, undergoes a reversal of the polymerization reaction after the initial breakage and yields mainly monomer molecules. Polyoxymethylene, poly-α-methystyrene, polytetrafluoroethylene belong to this group. These two groups of polymers undergo almost complete degradation while leaving hardly any

char (carbonized polymer residue). Polymers with reactive side groups attached to the backbone of a polymer chain may degrade initially as a result of interactions or instabilities of these groups; such reactions may then lead to scission of the backbone. Polyvinylchloride, PVC, and polyvinyl alcohol, PVA, are examples of such polymers. This group tends to undergo cyclization, condensation, recombination or other reactions which ultimately yield some char. Diene polymers, polyacrylonitrile, and many aromatic and heterocyclic backbone polymers also belong to this char-forming group. Common to the pyrolysis of all these polymers is the formation of conjugated multiple bonds, transition from a linear to a cross-linked structure, and an increase of the aromaticity of the polymer residue [12]. For polymers containing aromatic carbon- and/or heterocyclic links in the main chain of the polymer structure, general features of their pyrolysis and char yield have been derived [13,14]. Some features are: (1) The thermal stability and the char yield increase with the relative number of aromatic groups in the main chain per repeat unit of the polymer chain, (2) the thermal stability of heterocyclic polymers increases with the aromatic component of the heterocycles, (3) pyrolysis begins with the scission of the weakest bonds in the bridging groups connecting the aromatic rings or heterocycles. Char-forming thermoplastics often swell and intumesce during their degradation/combustion and one recent flame retardant approach promotes the formation of such intumescent char, as discussed later in this paper.

Degradation of a polymer is often affected by the presence of abnormal structures which are usually less thermally stable than the regular structures. Some such structures are inherent consequences of the method of polymerization. If a vinyl polymer is polymerized with a free radical initiator, termination reactions yield unsaturated end groups and also a head-to-head linkage within the chain. These abnormal structures were found in PMMA and it was shown that they lowered the thermal stability of the polymer and reduced ignition-delay time and increased the burning rate [15,16].

As described above, the type of polymer structure, thermal properties, and the amount of heat transferred to the polymer determine the depth over which the polymer is heated sufficiently to degrade. Since the boiling temperatures of some of the degradation products are much less than the polymer degradation temperatures, these products are superheated as they form. They nucleate and form bubbles. Then, these bubbles grow with the supply of more small degradation products by diffusion from the surrounding molten polymer [17]. Since the polymer temperature is higher near the surface than farther below, the polymer sample is more degraded there and its molecular weight, M, is lower. Since the viscosity of the molten polymer, η, depends strongly on molecular weight and temperature (for example, $\eta=cM^{3.4}$ or $\eta= \exp\{-M/(E(T-T_g))\}$ [18]), the viscosity near the surface is much less than that in the interior. The net result is a highly complex generation and transport of bubbles containing small molecules from the interior of the polymer melt outward through a strong viscosity gradient that heavily influences bubble behavior. A qualitative description of this complex transport process and its effect on gasification rate has been given in ref.19.

There are several types of theoretical models describing the transient gasification rate history of polymeric materials under specified external heat fluxes such as energy feedback from flames

discussed above. Although detailed thermal degradation reactions have been modeled [20-22], the models did not include any heat and mass transport processes in polymer samples. On the other hand, if heat transfer and mass transport processes were included [23, 24], the degradation reactions were approximated by a one-step global endothermic reaction for thermoplastics. For char-forming polymers, a minimum of two simultaneous global reactions, one for char formation and the other for formation of gaseous products, are used [25]. However, the majority of models used in the fire research field are based simply on condensed phase heat conduction with a unique pyrolysis surface temperature and heat of gasification for the sample. This approach (sometimes called a thermal model) requires only a few quantities describing the condensed phase and has been applied to thermoplastics and also extended to char-forming materials (Basically, it is assumed that the heat transfer characteristic time in the condensed phase is much longer than the degradation reaction time and the characteristic time of mass transport of degradation products through the sample.). For char-forming materials, a unique pyrolysis temperature is specified to form char and gaseous degradation products with a global heat of gasification [26]. The char layer is formed with a specified char yield from the pyrolysis and it remains inert.

Since the chemical composition of real end products is often not known, even the above global model might not be able to be applied without knowing the required information on the materials. Then, a more direct approach to characterize the condensed phase (and also some of the gas phase characteristics) of polymeric materials is used, such as the use of bench scale flammability test methods, for example, the Cone Calorimeter [ASTM E 1354] or the LIFT (Lateral Ignition and Flamespread Test, ASTM E 1321) to measure ignition delay time, heat release rate, combustion products and flame spread characteristics. Then, the effective thermal properties of the materials, pyrolysis temperature, and heat of gasification can be deduced from the results; these are key quantities for a thermal model.

Selected Cases of Polymer Combustion

Horizontal Slab Burning

The combustion of a horizontal slab of polymeric material burning while subjected to an external radiant source was modeled using the above described global approaches in the gas phase and in the condensed phase and the predicted results were compared with experimental data. The slabs had several different diameters and a finite thickness. Two different polymeric samples were burned, one was PMMA and the other was wood, Douglas fir. The global modeling of the gas phase for the two materials is the same except for values of the material combustion characteristics for the gas phase such as the stoichiometric constant, the heat of combustion, the soot volume fraction, and the combustion efficiency, which were specific to the material in question. The shape of the flame was approximated as a right cylinder and radiative feedback rate from the flame to the material surface was calculated by a mean beam length to represent the characteristic path length [27].

The condensed phase model was different for the two materials. For PMMA, the model was divided into three parts based on the experimentally observed trends: first the preheating period up to ignition, second the transition period from ignition until a steady pyrolysis surface temperature was obtained, and the third a gasification period. The second period began when the surface temperature reached the specified ignition surface temperature of 290 °C. Then, a critical mass flux at piloted ignition [28] was used to initiate flaming and the coupling between the gas phase feedback and the fuel mass flux. When the surface temperature reached the specified pyrolysis temperature of 400 °C, the surface temperature did not increase any more. Then, the absorbed heat feedback from the flame was spent to gasify PMMA with a specific global heat of vaporization and was also lost by conduction to the interior of the sample. The thermal properties of PMMA were taken from our previous study [29]. Comparison of the calculated surface temperature history with the measured result at an external radiant flux of 22.5 kW/m^2 is shown in Fig.5. The results show close agreement except during the transition period where the measured surface temperature increased much quicker than the calculated result. A comparison between the calculated mass burning rate and the measured results is shown in Fig. 6. The calculated results predicted the correct trend, such as the fact that the mass burning rate was higher for the larger diameter sample, although their predicted values were much less than the measured values. As discussed below, this discrepancy is mainly caused by the flame temperature calculation in the gas phase model. Both results show that the mass flux increased rapidly in the later part of the tests due to less heat loss from the unexposed surface to a calcium silicate board (with lower thermal conductivity than PMMA) used as a backing material in the experiment and approximated as an adiabatic boundary in the calculation. The numerical calculation was terminated when the remainder of the PMMA became less than 2 % of the original weight. Higher burning rates for the larger diameter sample are due to a higher heat release rate (total combustible fuel supply increased with the larger surface area) and consequently larger/taller flames were produced, which increased the radiative heat feedback rate to the PMMA surface.

For Douglas Fir, a global one-step degradation reaction was used in the condensed phase model to form char and to generate combustible degradation products. The kinetic constants and thermal properties of Douglas Fir and char were taken from Ref. 30. Its thickness was 1.9 cm. Similar to the model for PMMA, during the pre-piloted-ignition period the sample was exposed to only external radiant flux. Heat losses from the exposed hot surface to the environment were by re-radiation and convection and the unexposed surface was adiabatic. Upon reaching the minimum mass flux for piloted ignition, the exposed surface received heat flux from the flame as well as an external radiant flux. Heat loss from the exposed surface by radiation continued but convective loss ceased since the exposed surface started to receive convected heat from the flame. The comparison of calculated and measured mass burning rates is shown in Figs. 7a and 7b, for 0.1 m diameter and 0.6 m diameter samples, respectively. Mass flux sharply increased shortly after piloted ignition but it rapidly decreased after the formation of a char layer which has lower thermal conductivity than virgin wood. Thus, the surface temperature became higher and consequently re-radiation loss from the hotter surface increased. These figures show that the calculated results are reasonably close to the measured data but tend to be lower. This trend is consistent with the case for PMMA and further improvement in the flame temperature calculation

is needed. The uncertainty in the flame temperature calculation is primarily a result of the uncertainty in the amount of entrained air flow. At a late stage of burning, numerous cracks in the char layer were observed in the experiments. This increased the gasification rate of wood as the virgin wood layer was exposed to the external radiation and the heat feedback from the flame. Such a phenomenon was not included in this model.

Upward Flame Spread on a Wall

Flame spread up a vertical wall is a component of many fire scenarios; it is important to be able to predict whether a flame will spread up the wall or not (and, if so, how fast) when a small ignition source is located at the bottom of the wall. If the flame spreads partially, how far up will it go ? There are several relatively simple models to answer such questions using material parameters inferred from the Cone Calorimeter and LIFT or equivalent bench scale tests. Slightly more detailed models are also available [26,31][2] but the most simplified model [32] is used here to demonstrate how the flammability properties measured in the above tests can be used to predict upward flame spread phenomena. The advantage of this most simplified model is that an analytical solution can be derived and the physical factors influencing upward flame spread can be clearly identified. In this model, the movement of the pyrolysis front measured relative to the bottom of the wall, y_p, is expressed as [32]

$$\frac{y_p}{y_0} = \frac{(\alpha+1)}{\alpha} e^{\alpha\tau} - \frac{1}{\alpha} \qquad (4)$$

where $\alpha=k_t\dot{Q}''_{avg}$ -1, y_0 is the initial pyrolysis length due to the ignition source and $y_0=k_t\dot{Q}'_0$. The parameter k_t is a constant in the relation between the average flame tip height and the total heat release rate per unit width [33] and $\dot{Q}''_{avg}$ is the average heat release rate per unit area of the pyrolyzing material, $\dot{Q}'_0$ is the heat release rate of the ignitor per unit width, and $\tau\equiv t/t_{ig}$ where t_{ig} is the ignition delay time of the material at the average flame heat flux. The parameter α must be greater than zero in order for the upward flame spread process to accelerate, as shown in Eq.(4). The values of $\dot{Q}''_{avg}$ and t_{ig} are measured in the Cone Calorimeter and LIFT tests[3]. The comparison of the predicted results based on the above approach with the experimental data in the corner of a room is shown in Fig.8 [32]. A series of full scale room lining fire tests was performed at the Swedish National Tesing Institute [34]. The test scenario consisted of lining the walls and ceiling of the room (2.43 m x 3.66 m x 2.43 m in height with an opening of 2 m by 0.9 m) with a given material. A 0.17 m by 0.17 m propane sand burner was placed in the corner of the room. Initially, a 100 kW fire was allowed to burn in the corner. If this fire did not cause flame spread in 10 minutes, then the burner output was increased to 300 kW. Figure 8 shows that the predicted results using the materials characteristics determined by bench scale

---

2 There are more detailed models of flame spread but they are beyond the scope of this paper; generally, however, increased detail is in the gas phase instead of the condensed phase.

3 There is some uncertainty in this model regarding under what external flux these values should be measured.

tests as inputs to Eq.(4) with a prescribed ignition source agree reasonably well with the experimental data.

Flame Retardants

The fire safety of materials can be enhanced by increased ignition resistance, reduced flame spread rates, lesser heat release rates and reduced amounts of toxic and smoke products, preferably simultaneously. The use of more thermally stable polymers, of which many are available, might be a valid solution to these requirements but generally the cost of these materials is relatively high and, furthermore, their physical properties or processability may not be as desirable as those of less stable polymers. The most common approach to enhance fire safety performance is the use of flame retardant additives to inexpensive polymers (large volume commodity polymers such as PE, PP, PS, PVC, and so on). The additives must have a minimum impact on physical properties and product cost. Although halogenated flame retardants are highly effective for reducing the heat release rate of commodity polymers, the future use of these retardants faces some questions. Public perception of the environmental impact of recycling and combustion of certain halogenated flame retardants has become an issue in Europe [35,36].

Although there are many possible approaches to non-halogenated flame retardancy such as the use of aluminum trihydrate or magnesium hydroxide (both generate water and act as a heat sink), an interesting and promising approach is the formation of char; only the current status of this latter approach is discussed in this paper. There are three mechanisms whereby the formation of char reduces flammability: (1) part of the carbon (and hydrogen) stays in the condensed phase, thus reducing the amount of gaseous combustible degradation products evolved; (2) the low thermal conductivity of the char layer over the exposed surface acts as thermal insulation to protect the virgin polymer beneath [37]; and (3) a dense char acts as a physical barrier to gaseous combustible degradation products [38]. As described in ref.19, some polymers form char when degraded in a fire but others do not. In order to understand how to form char or to increase the amount formed, it is important to study the chemical and physical structure of char[4]. Reference 39 presents excellent work on detailed analysis of the residues formed from aromatic engineering polymers to determine their chemical structure. These results indicate that when BPA-PC and other aromatic polymers are heated, they lose most of their aliphatic groups resulting in predominantly protonated and unprotonated aromatic carbons in the residual char.

The physical structure of char has significant effects on polymer flammability. It is generally preferable to form an intumescent char (swollen char) having a cellular interior structure consisting of pockets of trapped gas [40]. The dominant protective role of an intumescent char is mainly via its thermal insulating capability [38,40] rather than an obstacle to the passage of

4 There are numerous publications on the formation and characterization of carbon. Although these publications are relevant to char, this subject is beyond the scope of this paper.

volatile and low-viscosity products into the gas phase because low-viscosity polymeric melts can rise through an intumescent char layer due to capillary forces [41].

The majority of commodity polymers do not form char during their combustion and current research seeks to determine how to form char from these polymers. This char forming approach is most successful when the polymer chars rapidly and early in the burning process. To be useful the charring process must be designed so that it occurs at a temperature greater than the processing temperature but before the polymer decomposition has proceeded very far. Our approach to char promotion is to investigate relatively inexpensive additives which form char from commodity polymers and to gain a fundamental understanding of the additive's char formation mechanism with the goal of optimizing the additive's performance. Recent studies of the flammability of polymers containing silicon based materials have shown these materials to be promising fire retardants, either as additives, in blends with organic polymers or in copolymers [42,43]. We have selected a combination of silica gel and potassium carbonate additives and determined their effects on flammability properties of commodity polymers[44]. The intention in using silica gel with K_2CO_3 was to devise a method of in-situ formation of silicon based fire retardants during combustion. The reaction of silica gel and organic alcohols in the presence of metal hydroxides has been shown to give multicoordinate organosiliconate compounds [45]. Instead of synthesizing these materials and then combining them with various polymers to evaluate their effect on polymer flammability properties, we envisioned the reaction occurring in the condensed phase of the pyrolyzing polymer beneath the burning surface, by combining a polyhydroxylic polymer, e.g. PVA or cellulose, with silica gel and K_2CO_3. If the indicated reaction shown in Fig. 9 occurred between the polymer and the additives it should crosslink the polymer and might assist in forming a silicon-oxy-carbide, SiOC, type protective char during combustion.

Polymers and additives used in this study were[5] silica gel (Fisher Scientific Co., 28-200 mesh), potassium carbonate, K_2CO_3 (Mallinckrodt, granular) polypropylene, PP (Scientific Polymer Products, Inc., Mw = 240,000 g/mole), polystyrene, PS (Scientific Polymer Products, Inc., Mw 45,000 g/mole), styrene-acrylonitrile, SAN (GE Polymers), polymethymethacrylate, PMMA (Du Pont, Elvacite), poly(vinyl alcohol), PVA (Scientific Polymer Products, Inc., Mn = 86,000 g/mole, Mw = 178,000 g/mole, 99.7% hydrolysed via NaOH aq method), nylon 6,6 (Rhone Poulenc) and alpha cellulose (Sigma Chemical Co., fiber, 99.5%). All were used as received. The additives were mixed with the polymers by grinding the powders together in a mortar and pestle (generally, total additive mass percentage was at most 10%). Cone samples were prepared by compression molding the powdered samples (40 g-55 g) into 75 mm x 7-8 mm disks using a Carver press with a heated mold (~22 MPa (10 tons) held for 3-5 minutes at 150 °C or at glass transition temperature).

---

5 Certain commercial equipment, instruments, materials, services or companies are identified in this paper in order to specify adequately the experimental procedure. This in no way implies endorsement or recommendation by NIST.

The flammability properties of these samples were measured in the Cone Calorimeter at an incident flux of 35 kW/m^2. The results are summarized in Table 1 for the polymers and polymers with the addition of silica gel and K_2CO_3 [44]. Assuming all additives remained in the polymer residue after the test, the char yield was determined as (polymer residue weight - initial additives weight)/initial total sample weight. Smoke extinction area was determined by the extinction measurement of a He-Ne laser beam through the combustion product exhaust duct divided by the exhaust volume flow rate and sample weight loss rate. This value tends to indicate the concentration of particulates in the combustion products. The results show that the additives enhance the formation of carbonaceous char even if the original polymer does not generate any char such as PP, PS and PMMA. The increases in carbonaceous char yield for PVA and cellulose is nearly a factor of 10. The reduction in peak heat release rate by the additives is quite significant, reaching about 50% for PP, PVA, cellulose, and nylon 6,6. A typical result for the reduction in heat release rate is shown in Fig.10 for PP. However, the heat of combustion is not significantly affected by the additives and also the concentrations of particulates and CO in the combustion products do not increase with the additives. These trends are significantly different from those for halogenated flame retardant additives. The results presented here clearly demonstrate that the flammability of a wide variety of polymers is dramatically reduced in the presence of relatively small concentrations of silica gel and K_2CO_3. However, we have only just begun to find the effects of the additives on flammability. We are planning to evaluate other types of basic materials (K_2CO_3 is hygroscopic) and the effects of particle size, internal pore size and silanol content of the silica gel on flammability.

The above results indicate that these additives appear to act in the condensed phase. In order to understand their effects on polymer pyrolysis, the chars of PVA with silica gel / K_2CO_3 (90:6:4) and PVA with silica gel only (90:10) isolated following combustion in the Cone calorimeter, were analyzed using several solid state ^{13}C NMR techniques. The spectra are shown in Figures 11 and 12 for the PVA with silica gel only (90:10) char and for the PVA with silica gel / K_2CO_3 (90:6:4) char, respectively. The normal CP/MAS ^{13}C NMR, shown in the middle of Figure 11, contains a broad resonance in the aromatic-olefinic region from 110 ppm to 150 ppm and two weaker broad signals in the aliphatic region, one centered at 20 ppm and the other at 35 ppm. This spectrum shows that the ratio of aromatic-olefinic (sp^2) carbon to aliphatic (sp^3) carbon is ~ 3:1. An interrupted decoupling (ID)-CP/MAS spectrum of this char, shown in the bottom spectrum in Figure 9, reveals only the non-protonated carbons which have cross-polarized. Comparison of the ID-CP/MAS spectrum (bottom) to the normal CP/MAS spectrum (middle) reveals that the downfield shoulder in the CP/MAS spectrum, centered at 135 ppm, is due to non-protonated aromatic-olefinic carbons. The result of subtracting the appropriate intensity of the ID-CP/MAS spectrum from the CP/MAS spectrum, so that the downfield shoulder is removed, is shown in the top of Figure 11. This difference spectrum (top) reveals that the narrower upfield portion of the aromatic-olefinic resonance, at 110 ppm -135 ppm, is due to protonated carbons. The ratio of non-protonated to protonated aromatic-olefinic carbons in the cross-polarized signal of this char sample is approximately 1 to 1. Comparison of the set of NMR data above with that for the char resulting from the pyrolysis of pure PVA reveals that the non-protonated to protonated aromatic-olefinic carbon ratio is 1:1 in both cases and that the chars appear to have almost identical structure [46]. However, the presence of silica gel in PVA reduces the peak heat

release rate from 609 kW/m^2, for pure PVA, to 250 kW/m^2. The presence of silica gel also increases the char yield from 5% to 27%. It appears that the silica gel does not change the type of char formed, since the chars have similar structure, but it does change the rate that it forms since the char yield is higher and the flammability is lower.

A similar series of spectra of the char from PVA with silica gel and K_2CO_3 (90:6:4) is shown in Figure 12. The normal CP/MAS spectrum (middle) contains the sharp carbonate resonance at 162 ppm and a broad resonance in the aromatic-olefinic region from 115 ppm to 150 ppm. In contrast to the spectra for PVA only or for PVA with silica gel (10%) there is little evidence of any aliphatic (sp^3) carbon. Comparison of the ID-CP/MAS spectrum (bottom) to the normal CP/MAS spectrum (middle) reveals, as was observed for pure PVA and for PVA with silica gel, that the downfield shoulder in the CP/MAS spectrum, centered at 135 ppm, is due to non-protonated aromatic-olefinic carbons. The result of subtracting the appropriate intensity of the ID-CP/MAS spectrum from the CP/MAS spectrum, so that the downfield shoulder is removed, is shown in the top of Figure 10. The difference spectrum (top) reveals that the upfield portion of the aromatic-olefinic resonance, at 115 ppm -135 ppm, is due to protonated carbons. The ratio of non-protonated to protonated aromatic-olefinic carbon in the spectrum of this char sample is approximately 1.5 to 1, i.e., this char contains a greater fraction of non-protonated aromatic-olefinic carbons than the char formed in the absence of K_2CO_3. To the extent that the cross-polarized signals in these materials reflect the sample-wide chemistries, these data indicate that the presence of the K_2CO_3 has increased the extent of carbon-carbon bond formation and therefore of crosslinking in the char. This may be the reason for the even lower flammability (peak heat release rate: 609 kW/m^2 for pure PVA; 250 kW/m^2 for PVA with silica gel; and 194 kW/m^2 for PVA with silica gel and K_2CO_3) and for the higher char yield in the presence of K_2CO_3 (char yield: 5% for pure PVA; 27% for PVA with silica gel; and 43% for PVA with silica gel and K_2CO_3).

We are also characterizing the residues formed from the combustion of the polymers discussed above using solid state ^1H, ^{29}Si, single pulse (more quantitative) ^{13}C NMR, and other techniques. Our recent ^{29}Si NMR measurement of the carbonaceous char of PVA in the presence of the additives showed no signal corresponding to presumed Si-O-C or Si-C bonds. Therefore, it is not clear at present how silica gel and K_2CO_3 enhance the formation of carbonaceous char from a wide variety of polymers.

Acknowledgments

The authors would like to thank Dr. Sergey Lomakin for making flame retardant samples, Mr. Jack Lee for Cone Calorimeter data, Dr. David L. VanderHart for use of the NMR facilities.

References

1. Hamins, A., Konishi, K., Borthwick, P., and Kashiwagi, T.. "Global Properties of Gaseous Pool Fires", accepted in the Twenty-Sixth Symposium (International) on Combustion which will be held in July, 1996 at Naples, Italy.

2. Hamins, A., Klassen, M., Gore, J. , Fischer, S.J., and Kashiwagi, T., *Combust. Sci. Tech.*, 97, p.37 (1994).
3. Modak, A.T., *Fire Safety J.*, Vol.3, Nos.2-4, p.177 (1981).
4. Zukoski, E.E., Kubota, T., and Cetegen, B., *Fire Safety J.*, Vol.3, Nos.2-4, p.107 (1981).
5. Delichatsios, M.A., "Air Entrainment into Buoyant Jet Diffusion Flames and Pool Flames", SFPE handbook of Fire Protection Engineering, NFPA, Second Edition, Section 2/Chapter 3 (1995).
6. Hasemi, Y. Fire Safety Science - Proceedings of the First International Symposium, Hemisphere, p. 87 (1986).
7. Qian, C. "Turbulent Flame Spread on Vertical Corner Walls", NIST-GCR-95-669, National Institute of Standards and Technology, 1995.
8. Choi, M.Y., Hamins, A., Rushmeier, H., and Kashiwagi, T., Twenty-Fifth Symposium (International) on Combustion, The Combustion Institute, Pittsburgh, p. 1471, (1994).
9. Mita, I., "Effects of Structure on Degradation and Stability of Polymers" in "Aspects of Degradation and Stabilization of Polymers" (edited by Jellinek, H.H.G.), Elsevier Scientific, Amsterdam, Chapt.6, 1978.
10. Kelen, T., "Polymer Degradation", Van Nostrand Reinhold, 1983.
11. Grassie, N. and Scott, G., "Polymer Degradation and Stabilization", Cambridge Univ. Press, 1985.
12. Factor, A., "Char Formation in Aromatic Engineering Polymers" in "Fire and Polymers" (edited by Nelson, G.L.), ACS Symposium Series 425, ACS, Washington, pp.274-287 (1990).
13. Krevelen, D. W., Polymer, 16:615-620 (1975).
14. Aseeva, R. M. and Zaikov, G. E., "Flammability of Polymeric Materials" in "Advances in Polymer Science", Vol. 70:172-229 (1985).
15. Kashiwagi, T. and Omori, A., Twenty-Second Symposium (International) on Combustion, The Combustion Institute, Pittsburgh, 1988, pp.1329-1338.
16. Kashiwagi, T., Omori, A., and Nanbu, H., Combust. Flame, 81:188-201 (1990).
17. Clift, R., Grace, J. R., and Weber, M. E., "Bubbles, Drops, and Particles", Academic Press, 1978.
18. Matsuoka, S. and Kwei, T. K., "Physical Behavior of Macromolecules" in "Macromolecules" (edited by Bovey, F. A. and Winslow, F. H.), Academic Press, 1979, p.346.
19. Kashiwagi, T. and Ohlemiller, T. J., Nineteenth Symposium (International) on Combustion, The Combustion Institute, Pittsburgh, 1982, pp.815-823.
20. Nyden, M. C., and Noid, D. W., J. Physical Chemistry 95:940-945 (1991).
21. Guaita, M., and Chiantoe, O., Poly. Degr. and Stab. 11:167 (1985).
22. Inaba, A., and Kashiwagi, T., Eur. Polym. J., 23:871-881 (1987).
23. Vovelle, C., Delfau, J., and Reuillon, M., Combust. Sci. Tech., 53:187-201 (1987).
24. Wichman, I. S., Combust. Flame, 63:217-229 (1986).
25. Kansa, E., Perlee, H. E., and Chaiken, R., Combust. Flame, 29:311-324 (1977).
26. Chen, Y., Delichatsios, M.A., and Motevalli, V., Combust. Sci. Tech., 88:309-328 (1993).

27. Siegel, R. and Howell, J.R., Thermal Radiation Heat Transfer, Hemisphere Publishing Corp., 2nd ed., New York, p. 669 (1981).
28. Kashiwagi, T. and Omori, A., Twenty-Second Symposium (International) on Combustion, The Combustion Institute, p. 1329-1338 (1988).
29. Steckler, K.D., Kashiwagi, T., Fire Safety Science - Proceedings of the Third International Symposium, Elsevier Applied Science, p. 895-904 (1991).
30. Atreya, A. "Pyrolysis, Ignition and Fire Spread on Horizontal Surface of Wood" Ph.D. Thesis, Harvard Univ., 1983.
31. Kulkarni, A. K., Kim, C. I., and Kuo, C. H., "Heat Flux, Mass Loss Rate and Upward Flame Spread for Burning Vertical Walls", NIST-GCR-90-584, NIST, November 1990.
32. Cleary, T. G., and Quintiere, J. G., Fire Safety Science - Proceedings of the Third International Symposium. Elsevier, 1991, pp. 647-656.
33. Saito, K., Williams, F. A., Wichman, I. S., and Quintiere, J. G., J. Heat Transfer, 111:438-445 (1989).
34. Sundstrom, B., "Full Scale Fire Testing of Surface Materials", Technical Report SP-RAPP 1986:45, Swedish National Testing Institute, Boras 1986.
35. Nelson, G.L., "Recycling of Plastics - A New FR Challenge", The Future of Fire Retarded Materials: Applications & Regulations, FRCA, p.135, October 1994.
36. Van Riel, H.C.H.A, "Is There a Future in FR Material Recycling; The European Perspective" ibid, p.167.
37. Anderson, C. E., Jr., Ketchum, D. E., and Mountain, W. P., J. Fire Science, 6:390-410 (1988).
38. Camino, G., Costa, L., Casorati, E., Bertelli, G., and Locatello, R., J. Appl. Polym. Sci., 35:1863-1876 (1988).
39. Factor, A., "Char Formation in Aromatic Engineering Polymers" in "Fire and Polymers" (edited by Nelson, G.L.), ACS Symposium Series 425, ACS, Washington, pp.274-287 (1990).
40. Scharf, D., Nalepa, R., Heflin, R., and Wusu T., Fire Safety J. 19:103-117 (1992).
41. Gibov, K. M., Shapovalova, L. N., and Zhubanov, B. A., Fire and Materials, 10:133-135 (1986).
42. Kashiwagi, T., Fire Calorimetry, Proceedings of a special symposium on Fire Calorimetry, Report # DOT/FAA/CT-95/46, p.48 (1995).
43. Buch, R.R., ibid, p.154.
44. Gilman, J.W., Kashiwagi, T. and Lomakin, S.M., 41st International SAMPE Symposium and Exhibition, Vol. 41, SAMPE, p.708-713 (1996).
45. Laine, R.M., *Nature*, 353:642 (1991).
46. Gilman, J.W., VanderHart, D.L. and Kashiwagi, T. in *Fire and Polymer II*, ACS Symposium Series 599, ed. by G.L. Nelson, p.161-171, American Chemical Society, Washington, D.C. (1995).

Table 1. Cone Calorimetry Data

Sample disk 75mm x 8mm	Char Yield (%)	LOI (%)	Peak RHR (Δ) (kW/m^2)	Mean RHR (kW/m^2)	Mean Heat of Combustion (MJ/kg)	Total Heat Released (MJ/m^2)	Mean Ext. Area (m^2/kg)	Mean CO yield (kg/kg)
PP	0	-	1,760	800	38	360	690	0.04
PP w/ 6%SG & 4%PC	10	-	740 (58%)	510	33	300	710	0.04
PS	0	18	1,740	1,010	25	280	1,420	0.07
PS w/ 6%SG & 4%PC	6	24	1,190 (31%)	720	25	250	1,500	0.07
PMMA	0	18	720	570	23	320	210	0.01
PMMA w/ 3%SG & 1%PC	15	25	420 (42%)	250	21	230	200	0.05
PVA	4	-	610	380	17	220	590	0.03
PVA w/ 6%SG & 4%PC	43	-	190 (68%)	110	12	100	200	0.03
Cellulose	4	-	310	160	11	100	30	0.02
Cellulose w/ 6%SG & 4%PC	32	-	150 (52%)	70	5	30	20	0.04
SAN	2	-	1,500	840	25	200	1,330	0.07
SAN w/ 6%SG & 4%PC	3	-	1,130 (25%)	770	23	170	1,300	0.06
Nylon 6, 6	1	30	1,130	640	23	110	230	0.02
Nylon 6, 6 w/ 3%SG & 2%PC	5	33	530 (53%)	390	22	100	170	0.02
Nylon 6, 6 w/ 6%SG & 4%PC	6	30	550 (52%)	370	24	100	180	0.02

SG = Silica Gel, PC = K_2CO_3

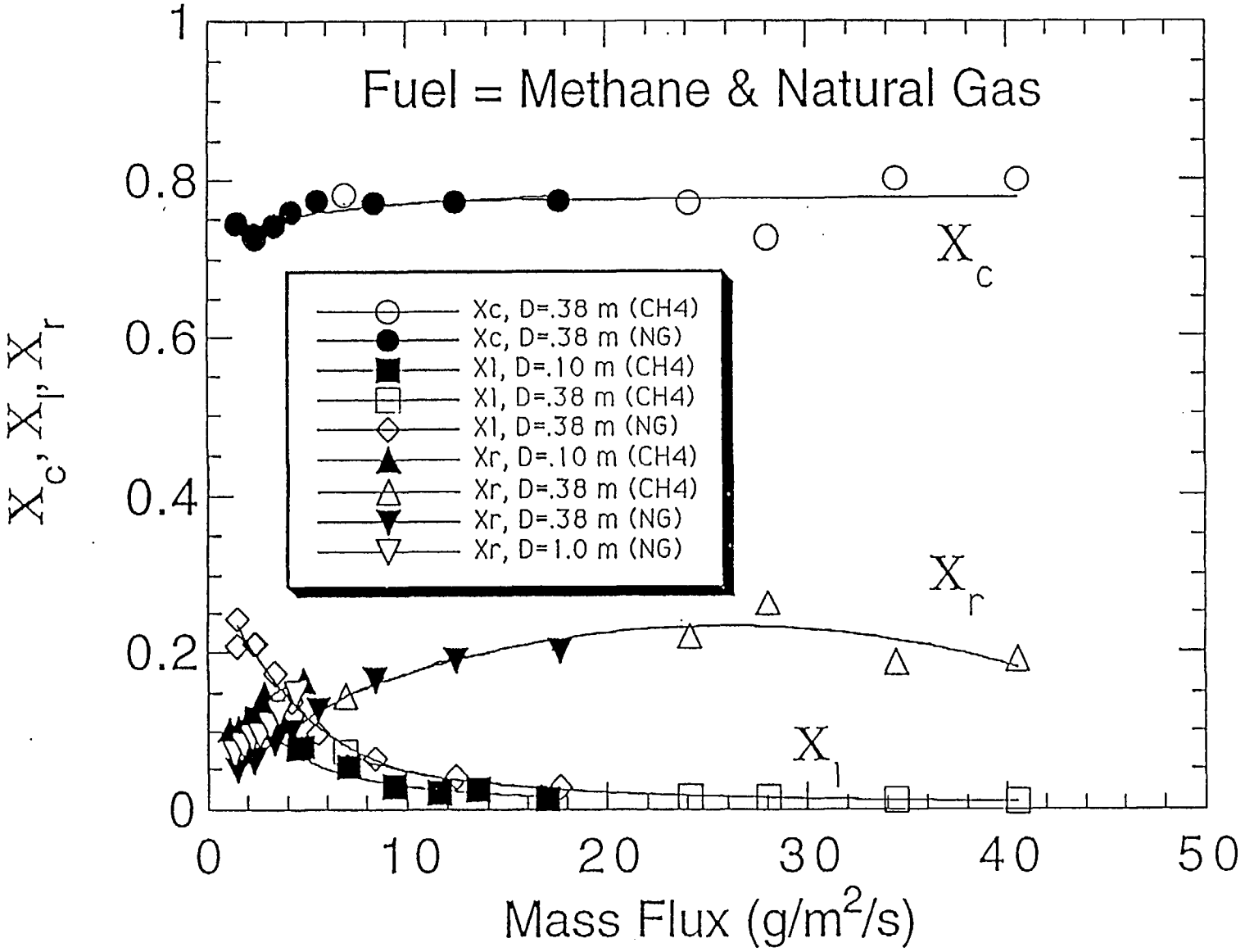

Figure 1. Fractions of idealized heat release dissipated by convection, radiation, and feedback to the fuel surface with respect to fuel mass flux for methane and natural gas. [ref.1]

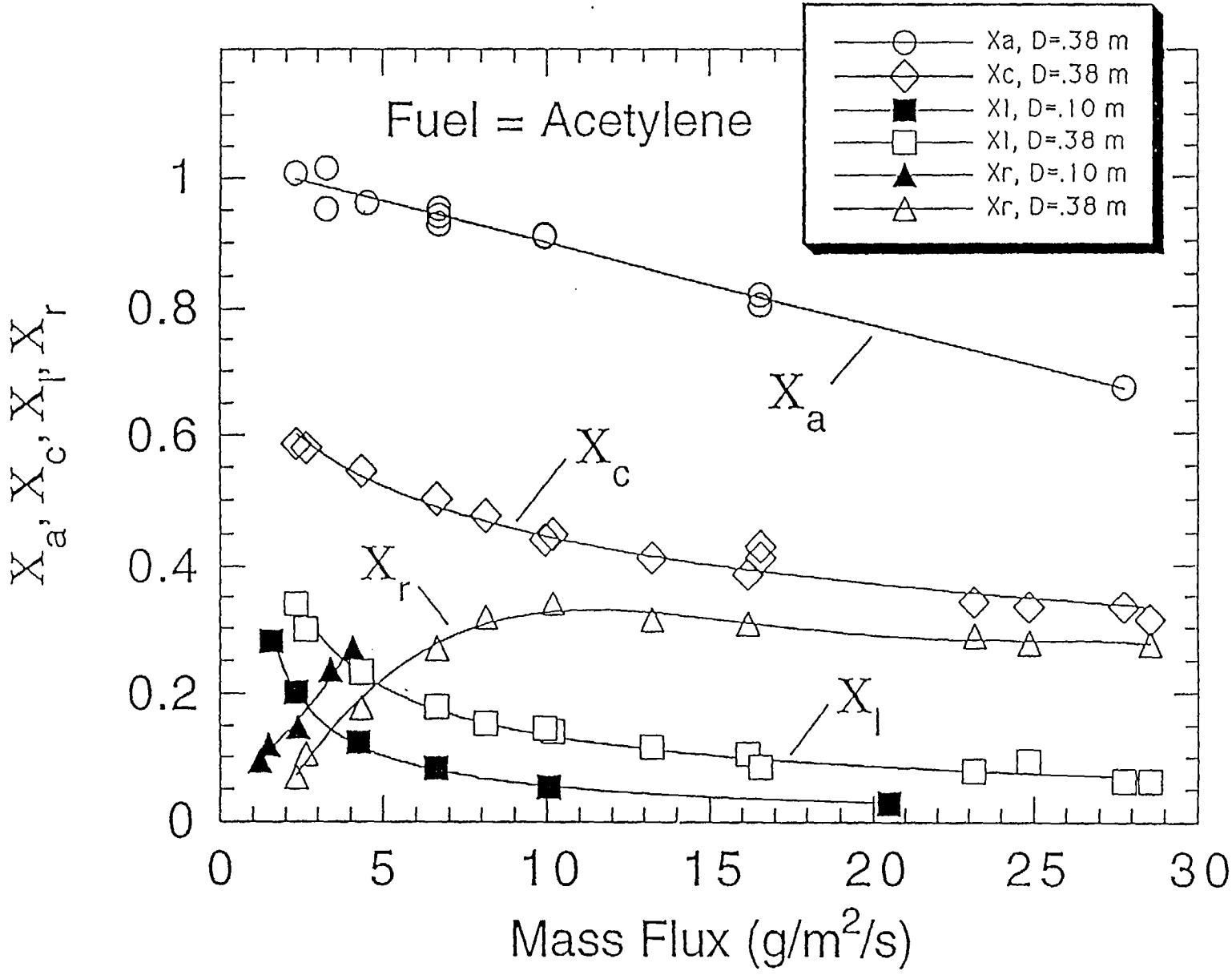

Figure 2. Fractions of idealized heat release dissipated by convection, radiation, energy feedback to the fuel surface and combustion efficiency with respect to fuel mass flux for acetylene. [ref.1]

Figure 3. Measured axial radiative feedback rate distribution for three different 30 cm diameter pool flames. [ref.2]

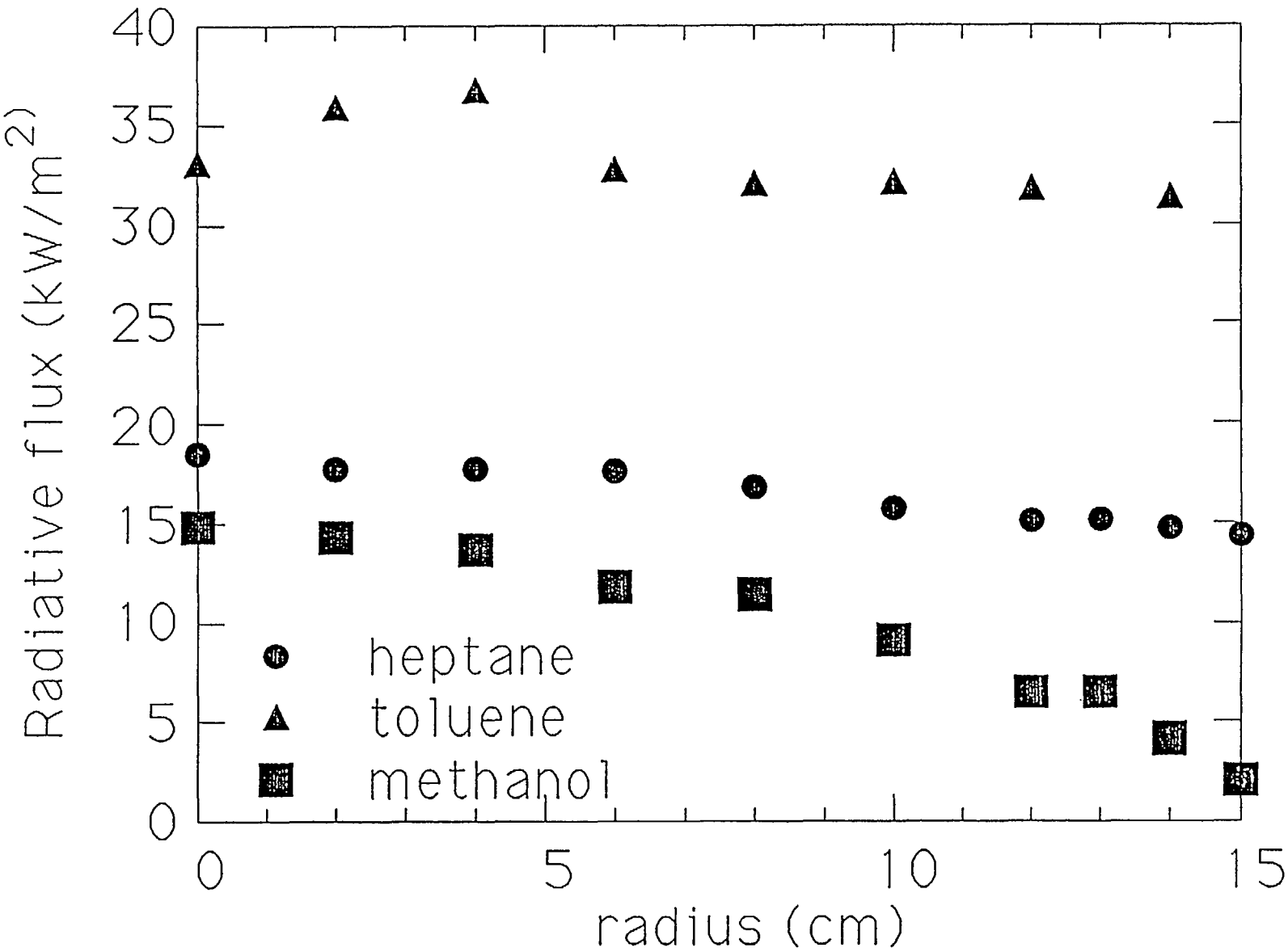

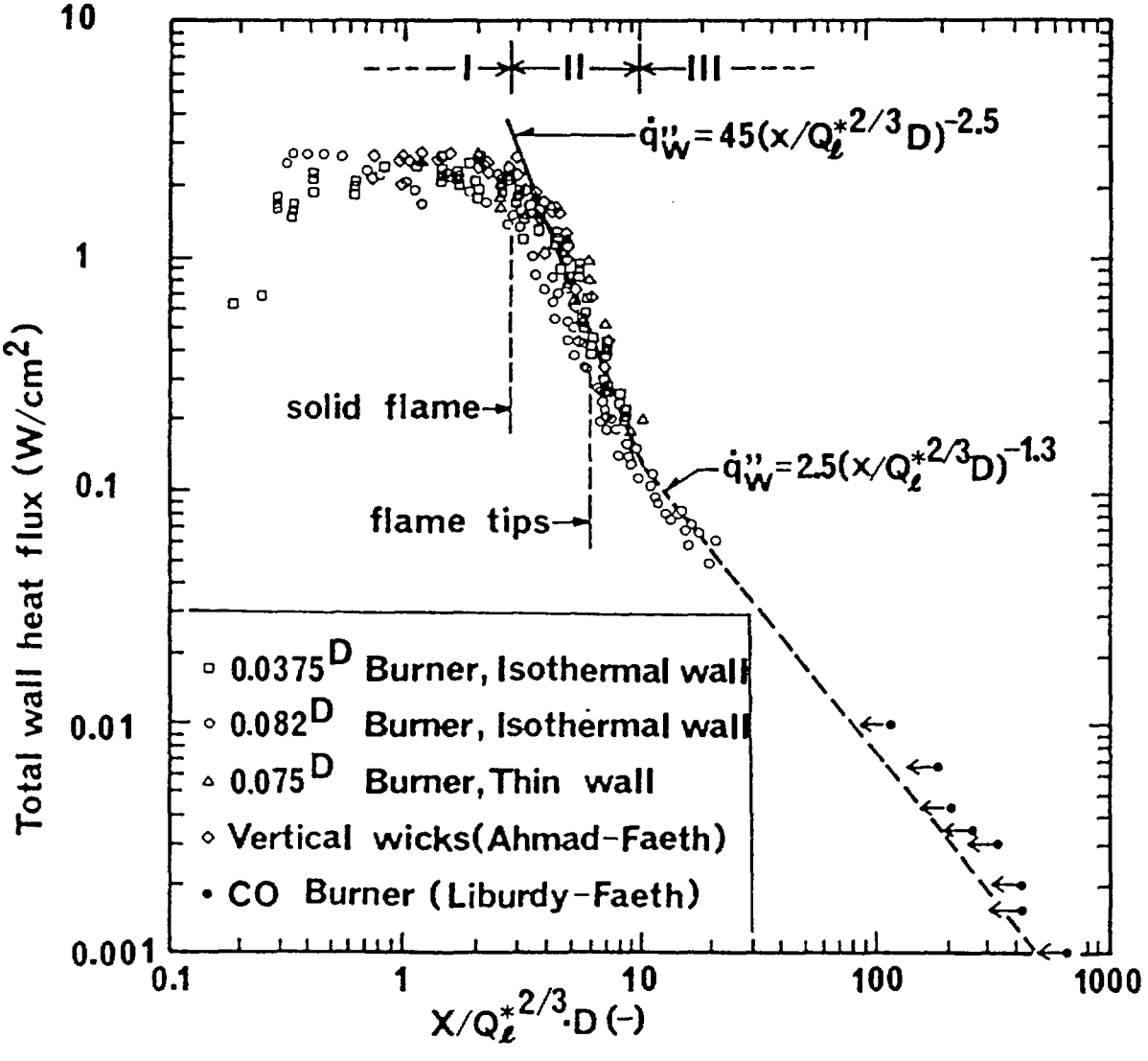

Figure 4. Measured correlation between energy feedback flux and normalized height. [ref.6]

Surface Temperature: PMMA

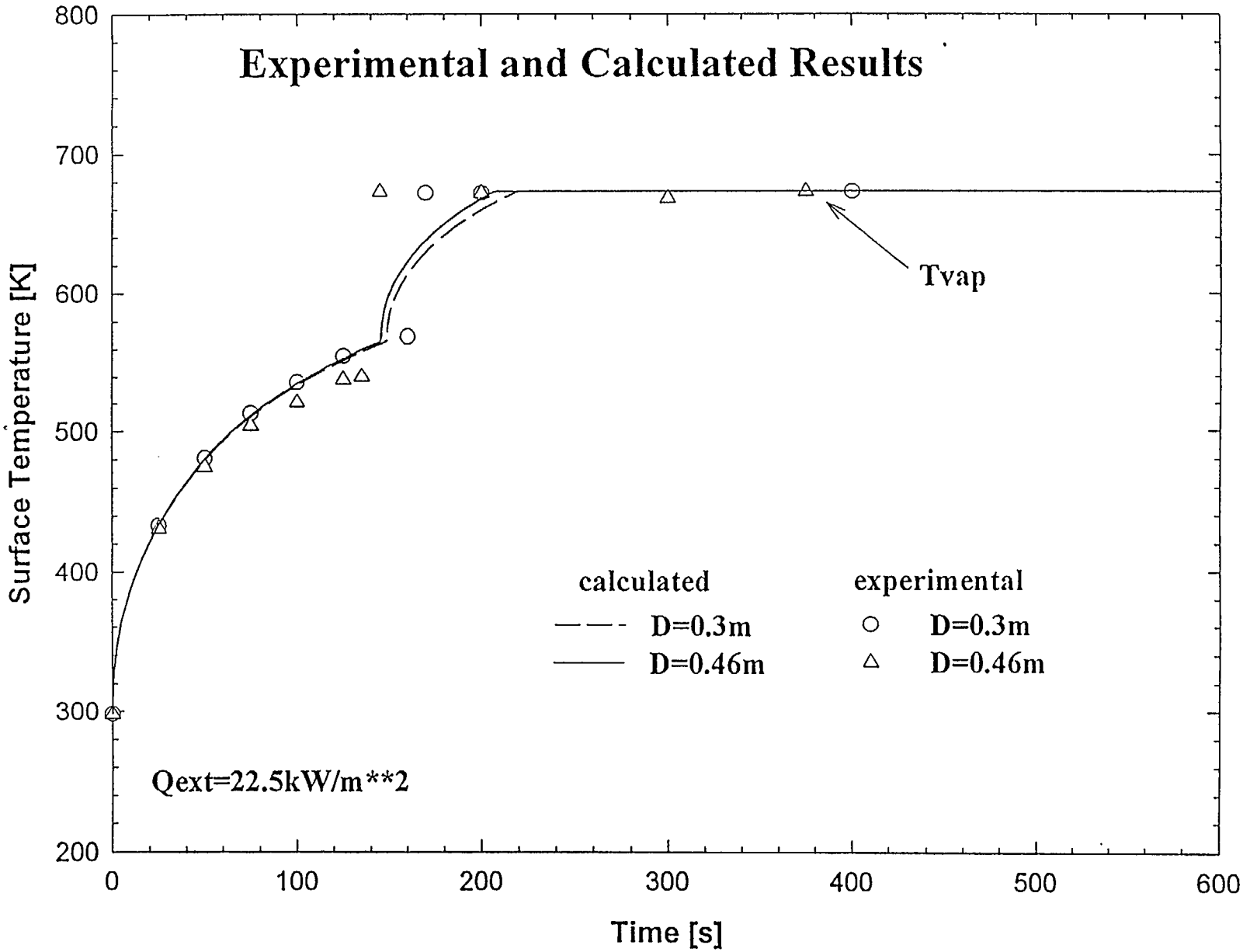

Figure 5. Comparison of of the calculated and experimentally measured surface temperature history of a circular PMMA slab sample (1.3 cm thick) for two different diameters.

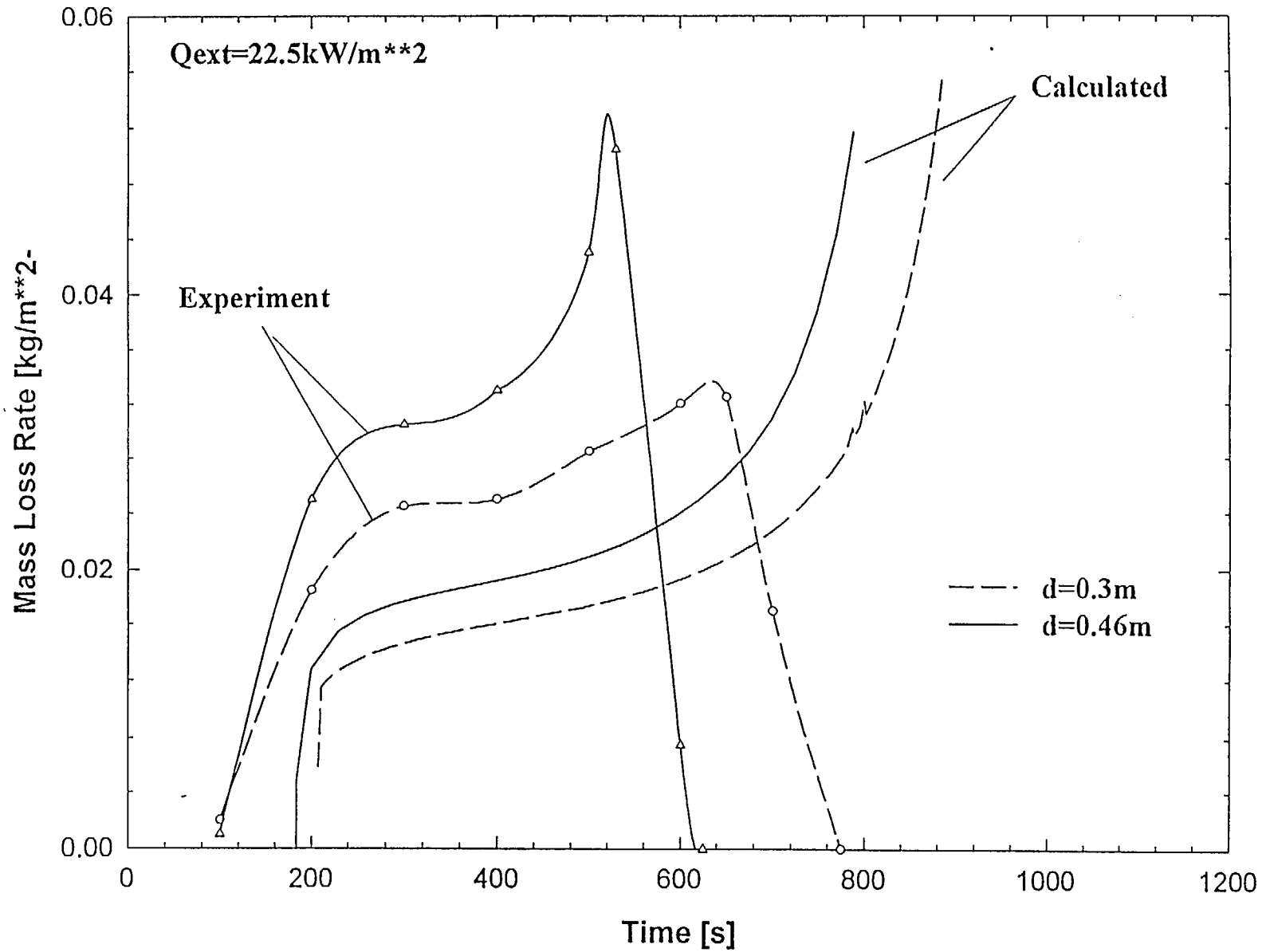

Figure 6. Comparison of predicted mass loss rate (burning rate) with experimental data for PMMA for two different diameters

Figure 7a. Comparison of predicted mass loss rate (burning rate) with experimental data for Douglas Fir (0.1 m diameter) at 25 kW/m^2

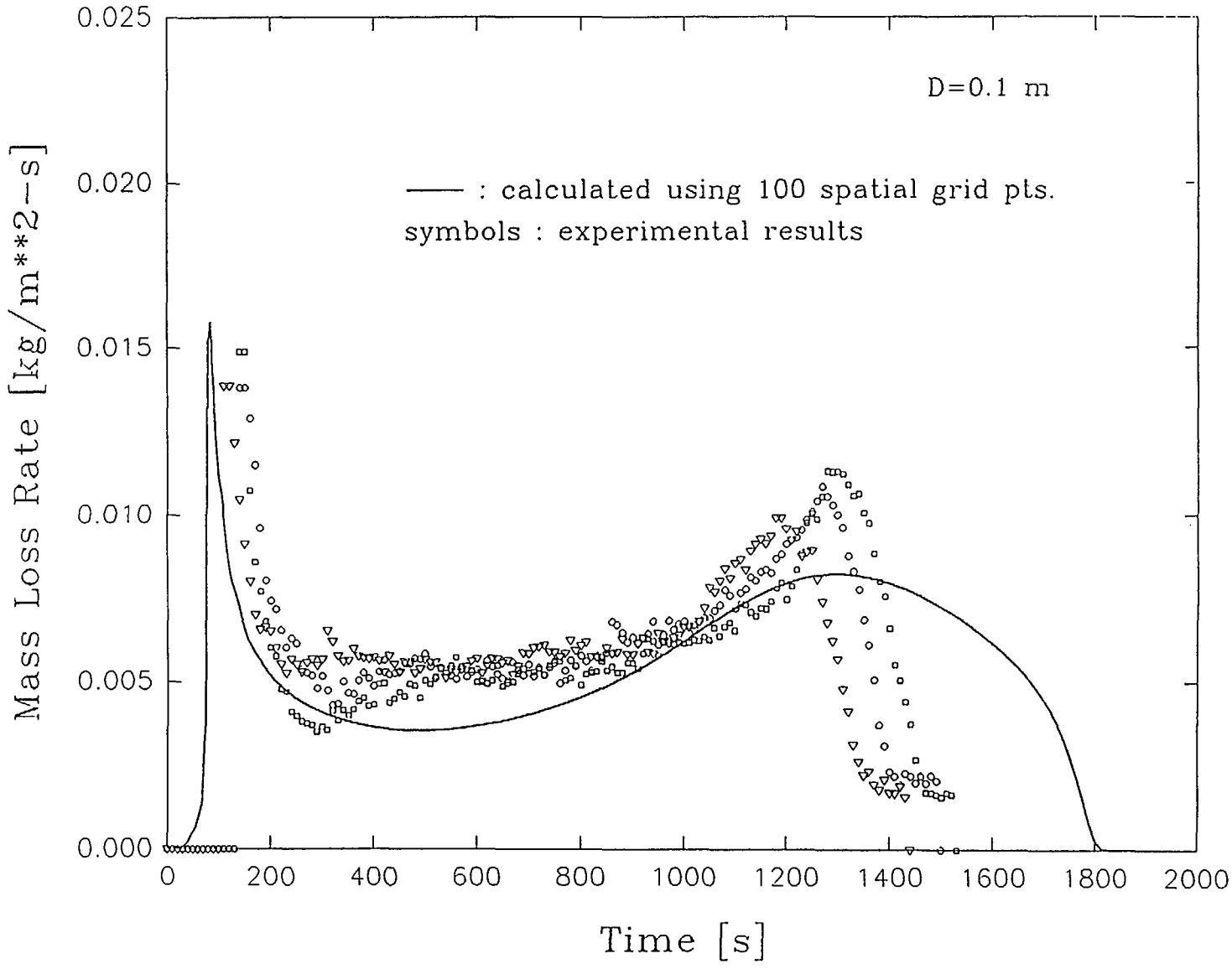

Figure 7b. Comparison of predicted mass loss rate (burning rate) with experimental data for Douglas Fir (0.6 m diameter) at 25 kW/m^2

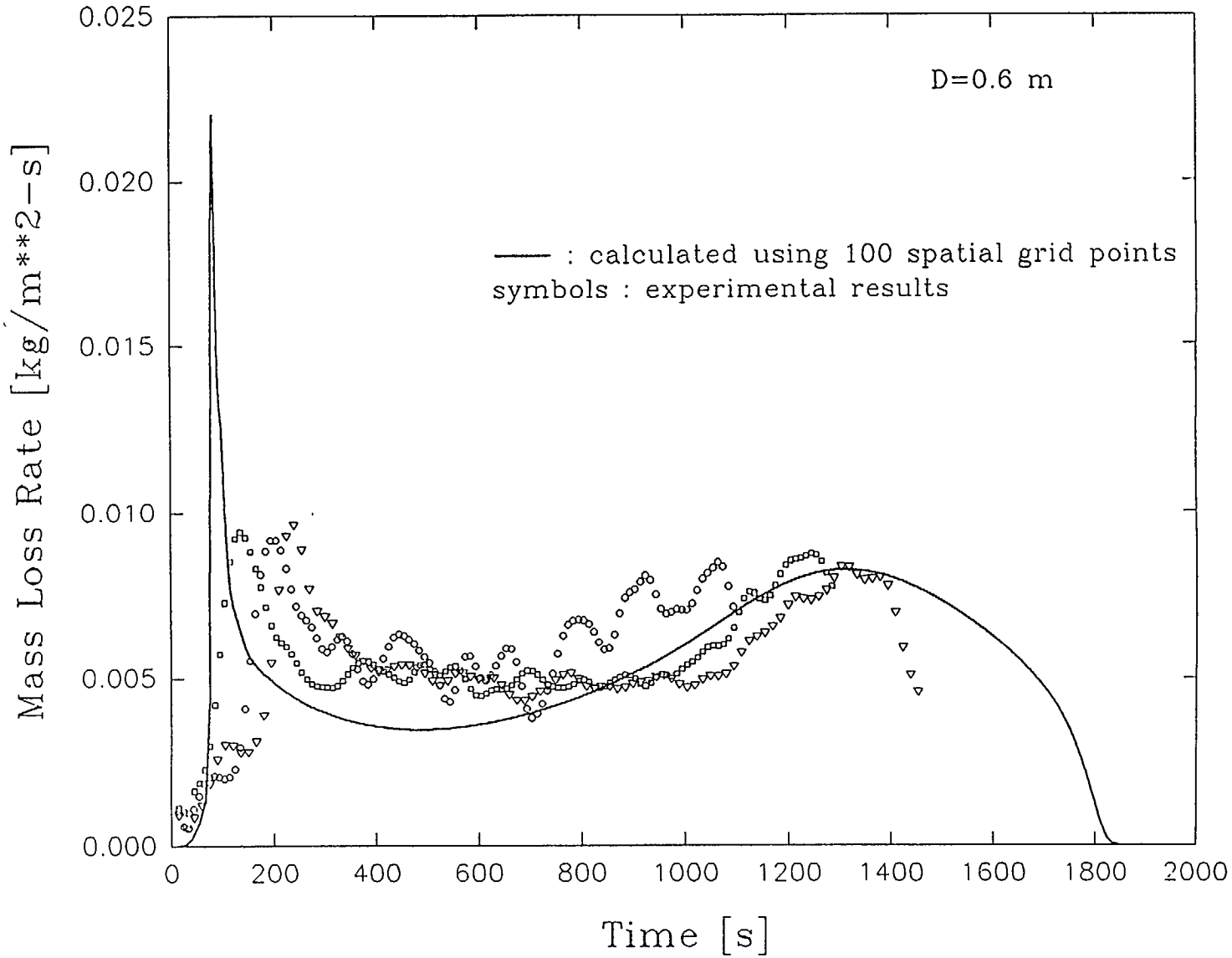

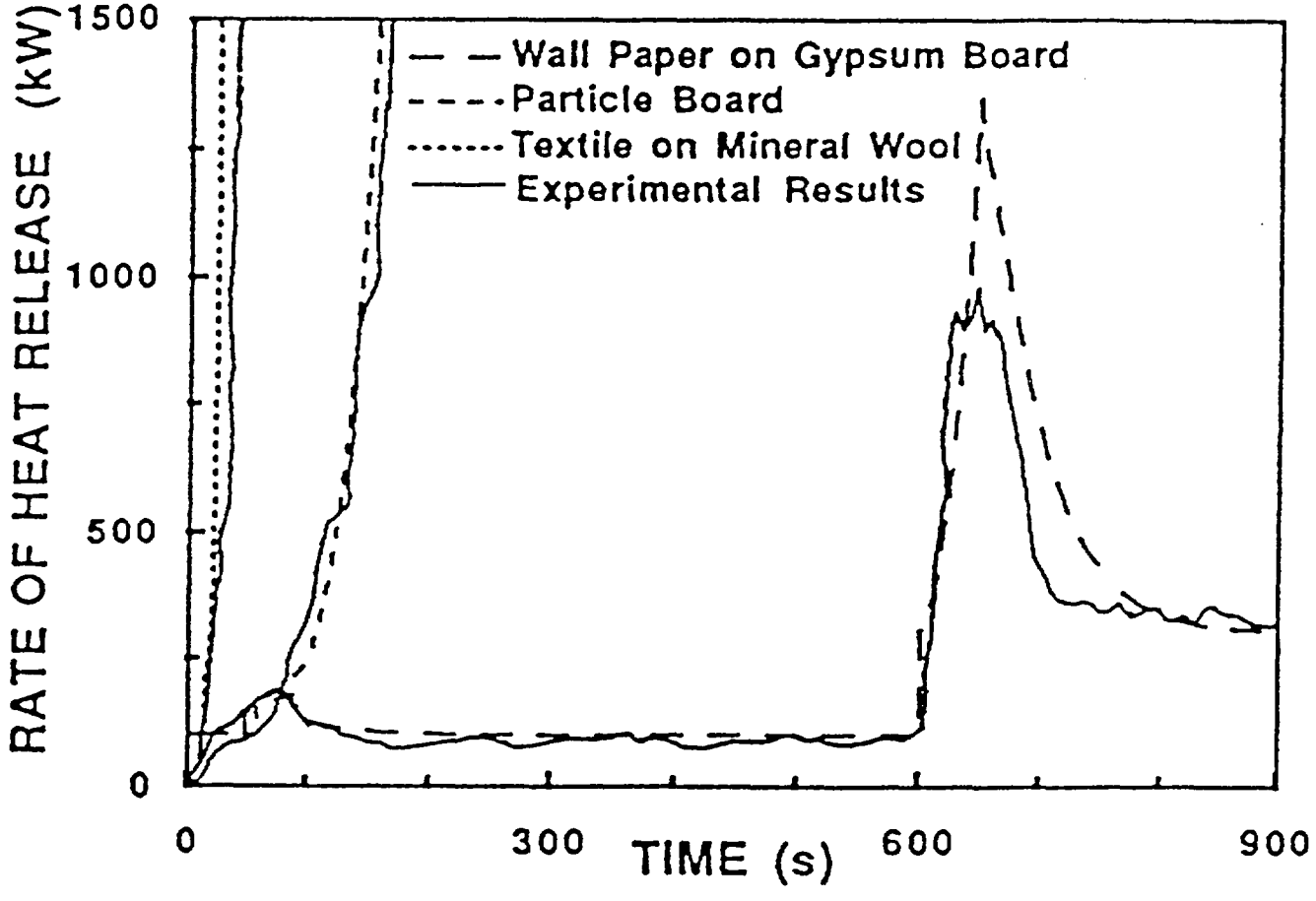

Figure 8. Comparison of predicted heat release rate with the experimental data during upward flame spread in the corner of a room. [ref.32]

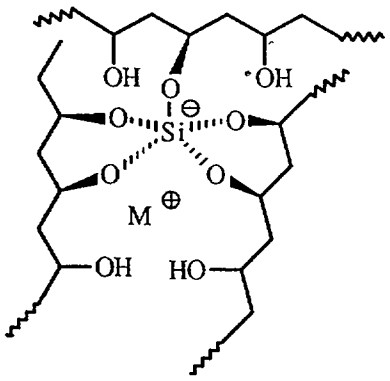

Figure 9. Pentacoordinate organosilicate crosslinked PVA. [ref.44]

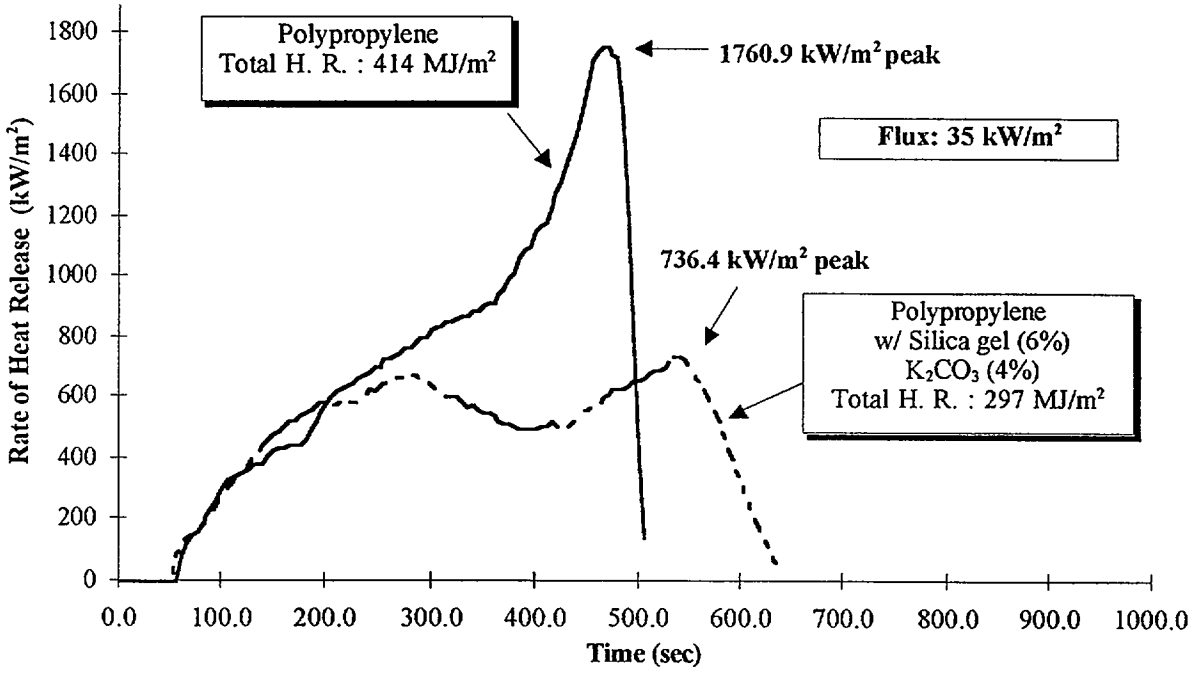

Figure 10. Heat release rate curves of PP (75 mm x 7 mm disk) and PP/silica gel/K_2CO_3 (90/6/4 ratio, 75 mm x 10 mm disk) with a 58% reduction in peak heat release rate and a 28% reduction in total heat release in the presence of the additives at 35 kW/m^2. [ref.44]

Figure 11. Solid state ^{13}C NMR spectra of char of PVA with silica gel only (90:10).

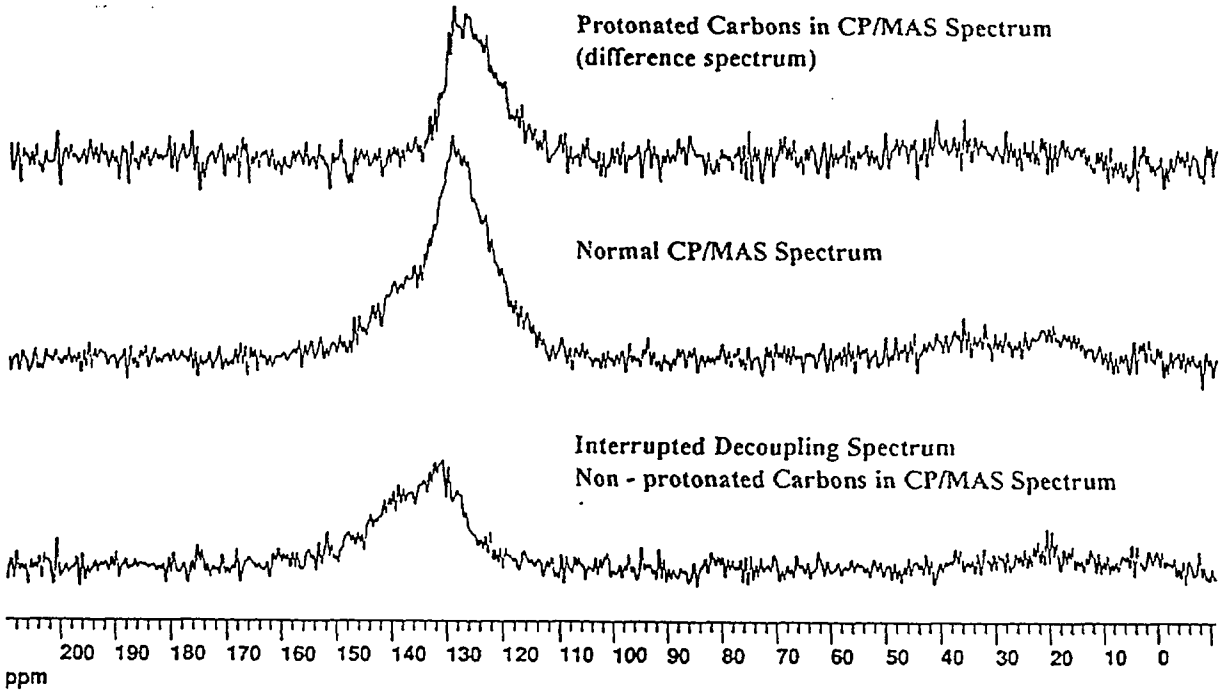

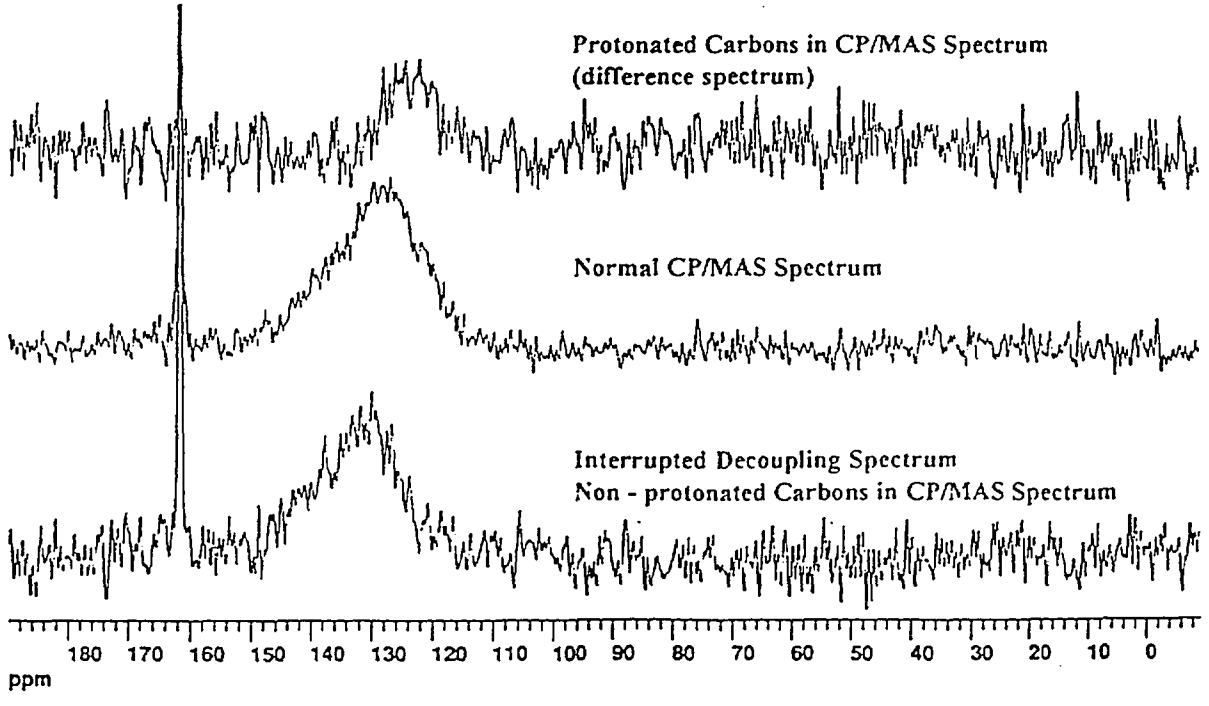

Figure12. Solid state ^{13}C NMR spectra of char of PVA with silica gel/K_2CO_3 (90:6:4).